# Natural Genome Diversity of AI-2 Quorum Sensing in *Escherichia coli*: Conserved Signal Production but Labile Signal Reception

Patrícia H. Brito[1],*, Eduardo P.C. Rocha[2,3], Karina B. Xavier[1,4], and Isabel Gordo[1]

[1]Instituto Gulbenkian de Ciência, Oeiras, Portugal

[2]Département Génomes et Génétique, Institut Pasteur, Microbial Evolutionary Genomics, Paris, France

[3]CNRS, UMR3525, Paris, France

[4]Instituto de Tecnologia Química e Biológica, Av. da República, Estação Agronómica Nacional, Oeiras, Portugal

*Corresponding author: E-mail: pbrito@igc.gulbenkian.pt.

## Abstract

Quorum sensing (QS) regulates the onset of bacterial social responses in function to cell density having an important impact in virulence. Autoinducer-2 (AI-2) is a signal that has the peculiarity of mediating both intra- and interspecies bacterial QS. We analyzed the diversity of all components of AI-2 QS across 44 complete genomes of *Escherichia coli* and *Shigella* strains. We used phylogenetic tools to study its evolution and determined the phenotypes of single-deletion mutants to predict phenotypes of natural strains. Our analysis revealed many likely adaptive polymorphisms both in gene content and in nucleotide sequence. We show that all natural strains possess the signal emitter (the *luxS* gene), but many lack a functional signal receptor (complete *lsr* operon) and the ability to regulate extracellular signal concentrations. This result is in striking contrast with the canonical species-specific QS systems where one often finds orphan receptors, without a cognate synthase, but not orphan emitters. Our analysis indicates that selection actively maintains a balanced polymorphism for the presence/absence of a functional *lsr* operon suggesting diversifying selection on the regulation of signal accumulation and recognition. These results can be explained either by niche-specific adaptation or by selection for a coercive behavior where signal-blind emitters benefit from forcing other individuals in the population to haste in cooperative behaviors.

**Key words:** genome evolution, gene loss, *E. coli*, balancing selection, social cheater, bacteria signaling.

## Introduction

There is an increasing awareness of the importance of microbial social interactions (Crespi 2001; West et al. 2006, 2007; Foster et al. 2007). Although unicellular organisms, bacteria can express complex coordinated multicellular behaviors, such as biofilm formation, antibiotic production, and secretion of virulence factors. Some of these behaviors require a large quorum of cooperating bacteria to be effective, that is, high cell density. Quorum sensing (QS) is a key communication system that coordinates cooperative behaviors in bacteria in function of cell density (Crespi 2001; Waters and Bassler 2005; Keller and Surette 2006; West et al. 2006).

QS involves the production, secretion, and recognition of small signal molecules called autoinducers detected by cognate receptors. Most autoinducers are species specific and thus promote intra-specific communication (Waters and

Bassler 2005). An important exception is the AI-2 system that uses as a signal a family of small molecules called autoinducer-2 (AI-2). The enzyme that produces AI-2 (LuxS) is present in both Gram-positive and Gram-negative bacteria. Because of the wide taxonomic distribution of LuxS, and the demonstration of the susceptibility of this system to interspecies interference, AI-2 has been proposed to be a signal produced to mediate both intra- and interspecies communication (Surette et al. 1999; Chen et al. 2002; Xavier and Bassler 2005a; Pereira, Thompson, et al. 2012). The substrate for AI-2 synthesis by LuxS is S-ribosylhomocysteine (SRH), which derives from the toxic intermediate S-adenosylhomocysteine (SAH) a product from S-adenosylmethionine (SAM) metabolism, an important and ubiquitous central metabolite of the cell (fig. 1) (Schauder et al. 2001; Winzer et al. 2002, 2003; Xavier and Bassler 2003; De Keersmaecker et al. 2006). For this
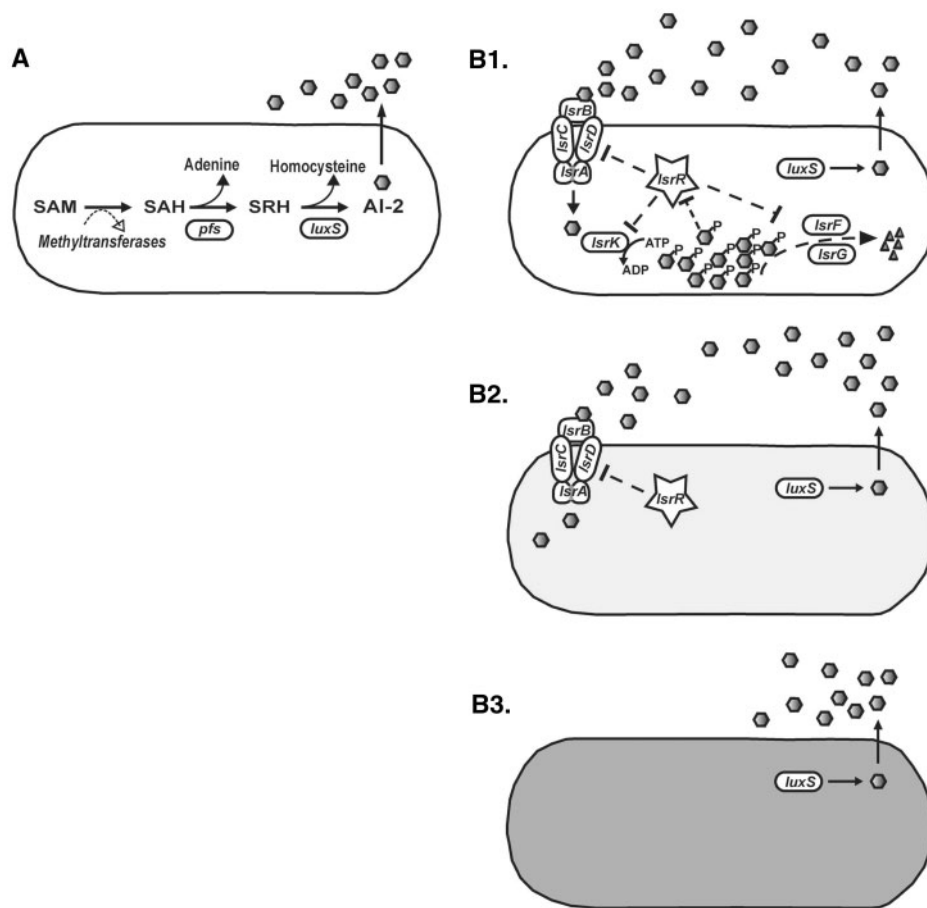
FIG. 1.—AI-2 biosynthetic pathway and Lsr-mediated transport and processing in *Escherichia coli*. (*A*) The precursor of AI-2 biosynthesis is SAM, an essential compound in central metabolism used as a methyl donor for DNA, RNA, and proteins. Following methyl transfer from SAM to its various substrates, the toxic compound SAH is formed. The Pfs enzyme removes adenine from SAH to form SRH. LuxS acts on SRH to produce homocysteine and AI-2 that released into the extracellular environment. (*B1*) AI-2 is bound by the periplasmic protein LsrB and internalized by the Lsr ATP-binding cassette transporter. Intracellular AI-2 is phosphorylated by LsrK, and the phosphorylated form of the signal (P-AI-2) induces *lsr* transcription by derepressing the repressor of the *lsr* operon (LsrR). This results in further assembly of the transporter and rapid AI-2 internalization. LsrF and LsrG proteins are also encoded by the *lsr* operon and are required for the further processing of intracellular P-AI-2. (*B2*, *B3*) Shaded cells represent examples of strains that maintain production of AI-2 although they lack the ability to sequester and process the extracellular AI-2 signal through the Lsr system (*B2*) or lack the Lsr system completely (*B3*). Pentagons represent the AI-2 signal.

reason, AI-2 can be considered a recycling product of SAM, and it has been suggested that it might not be a true signaling molecule in all AI-2-producing bacteria (Winzer, Hardie, et al. 2002; Winzer et al. 2002; Vendeville et al. 2005; Hardie and Heurlier 2008).

A major obstacle to understand the role of this molecule as a communication signal has been the lack of information on the molecular mechanisms of AI-2 detection and signal transduction networks in the majority of organisms. Importantly, such mechanisms have now been well characterized in *Escherichia coli* (reviewed in Pereira, Thompson, et al. 2012). In this bacterium, LuxS produces AI-2 during active growth, which is secreted into the extracellular medium where it accumulates in a cell-density manner until it triggers the activation of the Lsr (for LuxS regulated) system in the receptor cells. The genes of the *lsr* operon encode an ABC transporter

responsible for the internalization of AI-2 into the cells and other enzymes that regulate the expression of the operon and further intracellular metabolic degradation of the AI-2 signal (fig. 1). As a result of the activation of this system, AI-2 levels in the extracellular medium peak in midlate exponential phase and rapidly decline at the transition into stationary phase when the signal is removed from the environment (Wang, Hashimoto, et al. 2005; Wang, Li, et al. 2005; Xavier and Bassler 2005a, 2005b). By mediating the removal of AI-2 from the environment, this process can potentially affect any individual cell in the vicinity with AI-2-dependent gene expression, independently of its species identity (Xavier and Bassler 2005a; Pereira et al. 2008).

A recent study showed that the ability to bind and internalize AI-2 signal via Lsr is not ubiquitous among *E. coli* strains. Two *E. coli* strains were shown to lack many genes in the

operon, and phenotypic assays confirmed lack of function (Pereira et al. 2009). The finding of this unexpected polymorphism leads us to investigate the genetic diversity of the AI-2 system among *E. coli* natural populations. *Escherichia coli* is an important component of the mammalian gut microbiome, especially during lactation, and is extremely diverse. It comprises both commensal and pathogenic variants, with different tropisms, and even some environmentally adapted strains (Kaper et al. 2004; Tenaillon et al. 2010; Luo et al. 2011). The study of genetic variation in this species can thus provide important information on the role of the interspecies signal, AI-2, in an organism that coexists and interacts with many different species in its natural habitat. In *E. coli,* AI-2 QS regulates many social traits such as virulence (Zhu et al. 2007), biofilm formation (González-Barrios et al. 2006; Herzberg et al. 2006; Reisner et al. 2006; Lee et al. 2011), and chemotaxis and cell motility (Bansal et al. 2008; Hegde et al. 2011). If the fine tuning of AI-2 concentration via the LuxS production and Lsr system for AI-2 internalization is necessary to regulate the behavior of *E. coli* and of other species in the mammalian gut, the invasion of individuals that are impaired in signal production or internalization could affect the microbiota species composition and diversity. Such alterations of gut homeostasis can facilitate infections (Garrett et al. 2010; Clemente et al. 2012).

In this study, we analyze the genetic diversity of AI-2 production, detection, internalization, and processing at the gene content and nucleotide levels using all complete sequenced genomes of *E. coli* and *Shigella* natural strains. We use this information to determine whether selective processes are implicated in the evolution of this system. Many studies have addressed the biochemical mechanisms or the experimental evolution of QS. Oddly, there have been very few studies on the natural genome diversity of QS. Analyses of natural polymorphisms provide an important tool to understand the selective pressures acting on the evolution of social behaviors in microorganisms. The information provided by comparative genomics of natural organisms, which focus on polymorphisms that have passed the filter of natural selection through millions of generations in their natural habitats, are ideal to study the evolutionary relevance of genes and pathways. Here, we took advantage of the large number of genomes available from natural *E. coli* and *Shigella* strains to study from a genome-wide perspective the evolution of polymorphism of the different components of the AI-2 system. Our analysis reveals that the AI-2 system follows a unique pattern of genetic diversification that differs significantly from those of species-specific QS systems.

## Materials and Methods

### Genome Data

We retrieved all complete genomes of *E. coli* and *Shigella* spp. present in the Kegg database (http://www.kegg.jp/kegg/, last

accessed December 31, 2012) or in Genbank (http://www.ncbi.nlm.nih.gov/genome/, last accessed December 31, 2012). *Shigella* spp. genomes were included in the analysis because it is well accepted that these organisms belong to the *E. coli* species (Ochman et al. 1983; Pupo et al. 2000; Escobar-Páramo et al. 2003; Touchon et al. 2009). We excluded three laboratory strains for the following reasons: 1) *E. coli* str. K-12 substr. W3110 is a very recent laboratory variant of MG1655 (included in the study); 2) *E. coli* str. K-12 substr. DH10B; and 3) *E. coli* "BL21-Gold (DE3) pLysS AG" are genetically modified laboratory strains with closely related nonmodified strains in our data set (*E. coli* K-12 BW2952 [MC4100] and *E. coli* B REL606, respectively). We added *E. fergusonii* as it is an well-established outgroup of *E. coli* and *Shigella* strains (Lawrence et al. 1991). In total, we included 45 strains (supplementary table S1, Supplementary Material online), five of which are laboratory strains that were included in the phylogenetic reconstruction with the purpose of putting the natural strains and the natural diversification in the context of the better-studied laboratory strains. However, only natural strains were used in the population genetic analyses. All the genomes were downloaded on September 15, 2011. Gene content of the *lsr* operon was manually checked in each strain to confirm the presence of functional genes, identify misannotations, and characterize pseudogenes (identification of truncation, stop codon, and inserted sequences).

### Phylogenetic Analysis and Character Evolution

The list of orthologs between two genomes was identified using reciprocal best hits with more than 80% similarity in protein sequence and less than 20% difference in length, as in Rocha, Touchon, et al. (2006). The core genome of the clade was built using the intersection of lists of orthologs from the pairwise analyses. Each gene family in the core genome was aligned in protein sequence using MUSCLE (Edgar 2004) and then back-translated to DNA. The multiple alignments were concatenated, and phylogenetic reconstruction was performed on this alignment. A maximum likelihood distance matrix was built by Tree-puzzle 5.2 (Schmidt et al. 2002) under the Hasegawa–Kishino–Yano + $\Gamma$ model. The tree was inferred from the distance matrix using BIONJ (Gascuel 1997). Support of the topology was estimated by bootstrapping on the core genome concatenated alignment (100×).

To analyze character evolution, we coded each strain in terms of presence/absence of complete operon, pathovar, and the ability to replicate within macrophages. The latter two variables were coded using information from the literature. We traced the history of character change through the phylogeny with the program Mesquite version 2.75, build 566 (Maddison and Maddison 2011). Ancestral state reconstruction was made under maximum likelihood using an asymmetric Markov k-state two-parameter model, with rates estimated

from the data. Correlations were carried out with Pagel's 1994 test of independence between two binary characters (Pagel 1994) This test estimates the log-likelihood difference between a model where the rates of change in the two characters are independent and a model where the rates of change are correlated. The significance value of the log likelihood difference after 1,000 simulations is presented for each correlation.

## Character Simulations

We simulated character evolution along the phylogenetic tree to test whether the polymorphism observed for the presence/absence of a complete *lsr* operon evolves under neutrality. This corresponds to the null model. We evolved 1,000 categorical (binary) characters in Mesquite (Maddison and Maddison 2011) using the aforementioned two-parameter Markov-k model with asymmetric rates of forward and backward changes. Forward changes depict the instantaneous probability of gene inactivating mutations leading to incomplete, thus nonfunctional operon (from state 0 to state 1), and backward changes describe the instantaneous rate probability of regaining a functional operon, by back mutation, by gene conversion, or lateral gene transfer (from state 1 to state 0). To initiate the simulation process, one has to set the character frequencies at the root of the tree. We assumed those frequencies to be at equilibrium (rather than the alternative of equal frequencies). With this option, the expected frequencies at the root are assumed to be consistent with the model's rates, which is a more suitable option when the simulating model contains asymmetrical rates (Schluter et al. 1997). In this analysis, we calibrated the branch lengths of the phylogeny into the same units of the model parameters by considering the coalescent expectation that the time to the most recent common ancestor is in the order of $2N_e$ generations (Hudson 1990). Considering $\theta = 2N_e\mu$ and for *E. coli* $\theta = 0.0187$ estimated with the core genome (this study) and $\mu = 8.9 \times 10^{-11}$ (Wielgoss et al. 2011) can time to the most recent common ancestor to be approximately $2.11 \times 10^8$ generations, which corresponds to 0.0124 total branch lengths as estimated directly from the tree.

The simulations were carried out with rate parameters compatible with neutrality and with rate parameters estimated from the actual data. For each model, we estimated the level of polymorphism generated as the relative frequency of state 0 (functional operon), and the two distributions were tested for significant differences with a two-sample Kolmogorov–Smirnov test in R (http://www.R-project.org/, last accessed December 31, 2012).

## Genetic Diversity and Levels of Selection

Standard analyses of genetic diversity and neutrality tests (Tajima 1989; McDonald and Kreitman 1991; Stoletzki and Eyre-Walker 2011) were carried out for each gene with DnaSP

5.10 (Librado and Rozas 2009) and Mega4 (Tamura et al. 2007). McDonald–Kreitman test detects selection on protein coding sequences by comparing divergence and polymorphism data on synonymous and nonsynonymous sites under the assumption that synonymous substitutions are neutral; the test is robust to complex demography (Nielsen 2005) such as those likely to occur in bacteria. Tajima's *D* compares two measures of population genetic diversity that can be used to infer events of selection; but unlike the previous test, Tajima's *D* is highly sensitive to demographic effects (Simonsen et al. 1995). The number of synonymous (nonsynonymous) substitutions per synonymous (nonsynonymous) sites was estimated in MEGA4 (Tamura et al. 2007) using the modified Nei–Gojobori method that assumes a transition/transversion rate bias and uses a Jukes–Cantor correction to account for multiple substitutions at the same site. Standard errors were estimated after 1,000 bootstrap replicates. Patristic distances among strains were estimated in Mesquite (Maddison and Maddison 2011) by calculating the path-length distance from one strain to another along branches of core genome tree of figure 2.

We analyzed codon-specific selection in the two genes with significant McDonald–Kreitman tests. We estimated the rates of nonsynonymous and synonymous changes at each site using likelihood-based approaches as implemented in HYPHY package and made available through the Datamonkey web service (Kosakovsky Pond and Frost 2005). We made separate analyses with the fixed effects likelihood methods (FEL and iFEL) and with the random effect likelihood method (REL) (Pond and Frost 2005). iFEL is the "population-level" version of FEL and applies when one is interested in selective pressures that are restricted to interior branches of the tree (Kosakovsky Pond et al. 2006). REL tends to be more powerful than FEL but has a higher rate of false positives (Pond and Frost 2005). For this reason, we run all methods and compared the results. A Bayes factor of 20 or more in favor of $d_N > d_S$ is usually considered as providing strong support for adaptive selection at the site (Pond and Frost 2005). For all these analyses, we estimated for each data set the best-fitting nucleotide model and the gene phylogeny using the available options on Datamonkey.

We characterized codon usage of all genes using several statistics and averaging results across genomes: the effective number of codons (Wright 1990), the Codon Bias Index (Morton 1993), and the Codon Adaptation Index (CAI; Sharp and Li 1987). We used as a reference set the codon usage of a set of highly expressed genes in *E. coli* (Sharp and Li 1986). Expected value of CAI (eCAI) provides a direct threshold value for discerning whether the differences in CAI are statistically significant or whether they are merely artifacts that arise from internal biases in the G+C composition and/or amino acid composition of the query sequences (Puigbò et al. 2008). E-CAI is calculated from a set of query sequences by generating random sequences with G+C and amino acid
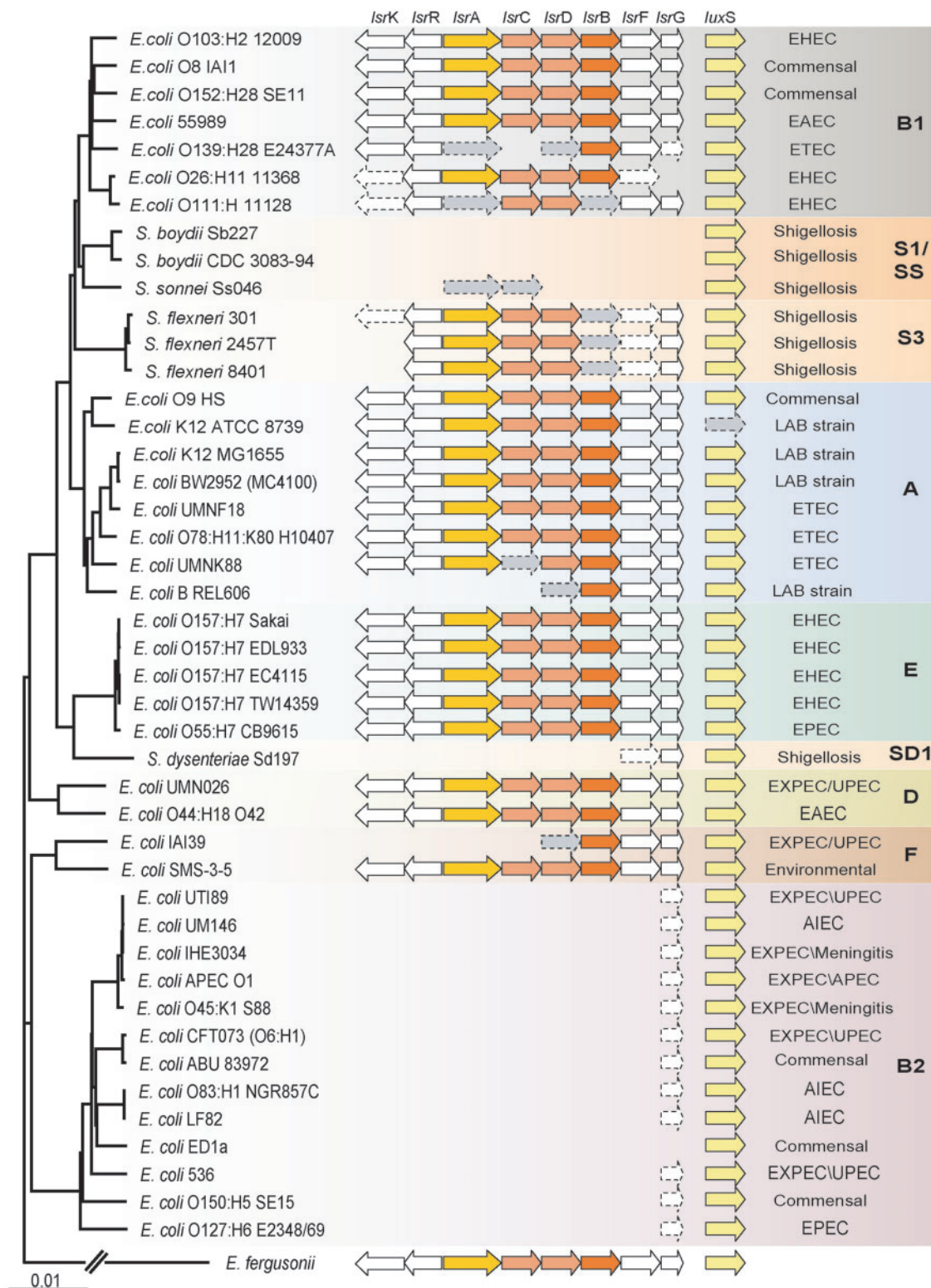
GBE



**Fig. 2.**—The phylogenetic analysis of *Escherichia coli* and *Shigella* strains inferred with the core genome (1,524 genes, 1.6 Mb). The tree was inferred by neighbor-joining based on the maximum likelihood distance matrix (see Materials and Methods). *Escherichia fergusonii* was used as the outgroup. Arrows indicate presence/absence of luxS and genes in the *lsr* operon. Dashed lines represent pseudogenes. On the right, pathovar and phylogroups are indicated. Pathovars are enteroaggregative *E. coli* (EAEC), enterohemorrhagic *E. coli* (EHEC), enterotoxigenic *E. coli* (ETEC), enteropathogenic *E coli* (EPEC), adherent invasive *E. coli* (AIEC), extraintestinal pathogenic *E. coli* (EXPEC), uropathogenic *E. coli* (UPEC), and avian pathogenic *E coli* (APEC).

content similar to those of the input. ENC and CBI were estimated with DNAsp, and eCAI was estimated the E-CAI server available at http://genomes.urv.es/CAIcal/E-CAI (last accessed December 31, 2012).

## Phenotypic Characterization of Null Mutants

Wild-type *E. coli* K-12 strain MG1655 (Blattner et al. 1997) was used as the parental strain (supplementary table S2, Supplementary Material online). To construct chromosomal single-gene deletions, kanamycin resistance cassettes from the Keio collection of single-deletion mutants (obtained from National BioResource Project [Japan] [Baba et al. 2006]) were introduced in the desired gene by phage P1 transduction from the Keio collection to MG1655, as described elsewhere (Silhavy et al. 1984). All deletions were confirmed by polymerase chain reactions using Taq DNA polymerase (New England Biolabs).

The phenotypes of all single-deletion mutants were determined in terms of AI-2 internalization by quantifying the time course of extracellular AI-2 concentration in cell-free supernatants. Bacteria were grown at 37°C with aeration in Luria–Bertani (LB) broth. To measure AI-2 concentrations, we followed the protocol described in Taga and Xavier (2011). Briefly, we diluted overnight cultures (1:100) into fresh LB medium and periodically collected aliquots of which we measured both optical density (OD600) and AI-2 concentration using the in vitro assay based on the CLPY-FRET method (Taga and Xavier 2011).

## Results

### Diversity of the Gene Repertoire of AI-2 QS

The phylogenetic relationship among *E. coli* and *Shigella* strains was inferred with the core genome of all strains including the outgroup (fig. 2). Every node in this phylogeny has 99–100% bootstrap support with the exception of two small internal nodes, one within the phylogroup B1 with 92% and another within B2 with 56%. This phylogeny shows the same phylogroups as previous studies (Touchon et al. 2009). The core genome of the clade (*E. coli* + *E. fergusonii*) is only of 1,524 genes corroborating previous conclusions that no single strain can be regarded as highly representative of the species and justifying the need for including gene repertoire variation in population genetic studies of *E. coli*.

Figure 2 shows a remarkable pattern of presence/absence polymorphism of the AI-2 regulated *lsr* genes among all sampled 44 strains of *E. coli* and *Shigella*. Many strains lack a complete *lsr* operon, but all natural strains encode the AI-2 synthase (*luxS*) (these results do not change with the addition of 13 new complete genomes that became available during manuscript revision). The frequency of the complete operon is 38%. This intermediate frequency is very rare in *E. coli*, where most gene families are at frequencies higher than 90% or

lower than 20% (Touchon et al. 2009). The close similarity in topology between the phylogenetic tree built with the sequences of the genes in the *lsr* operon and the species tree reconstructed with the core genome (supplementary fig. S1, Supplementary Material online) indicates that although recombination and lateral transfer cannot be ruled out, the prevalent phylogenetic signal in this locus is one of the species. Hence, the simplest explanation for the observed polymorphic pattern is that the operon is ancestral to all *E. coli,* and we can therefore use the presence/absence of genes to infer ancestral states. A maximum-likelihood reconstruction of ancestral states for the presence/absence of a completely functional *lsr* operon suggests that the operon was present in the last common ancestor of all *E. coli* (including *Shigella*) (proportional likelihood = 0.60, this is the scaled likelihood, so that the likelihood of both states add to 1). This is further supported by the taxonomic distribution of the *lsr* operon, which is found in many Gammaproteobacteria, including most close relatives of *E. coli* such as *E. fergusonii* and the new *E. coli* clades that are outside the "typical" *E. coli* strains (Luo et al. 2011; Oh et al. 2012). This operon is also found in the close genus of *Salmonella*, *Yersinia*, *Enterobacter*, and *Klebsiella*. Hence, *lsr* genes lacking in extant *E. coli* genomes are most likely the result of gene losses.

We observed no significant correlation between the presence/absence of a complete *lsr* operon and pathogenicity in general (Pagel's 1994 test, $P = 0.449$). However, the pathovars that are known to replicate within macrophages—all *Shigella* and all adherent invasive *E. coli* (AIEC) strains (Glasser et al. 2001)—lack the full *lsr* operon (Pagel's 1994 test, $P = 0.048$). The majority of EXPEC strains investigated here (seven of eight) also lack the full operon (Pagel's 1994 test, $P = 0.080$). EXPEC strains are extraintestinal pathogenic *E. coli* that are part of a healthy intestinal microbiota but can become virulent in extraintestinal environments (Wold et al. 1992; Nowrouzian et al. 2005; Moreno et al. 2009). These results suggest association between patterns of polymorphism at the *lsr* operon and relevant phenotypic traits differentiating *E. coli* strains.

### Processes of Pseudogenization

To gain further insight on the process leading to loss of the *lsr* operon, we studied its patterns of pseudogenization. The maximum-likelihood reconstruction of ancestral states suggests the occurrence of at least eight independent losses of function in the *lsr* operon during the evolution of the *E. coli* clade (supplementary fig. S2, Supplementary Material online). Once initiated, the process of pseudogenization is fast and does not follow a fixed gene order. For instance, closely related strains such as the ones in phylogroup B1 can differ substantially in presence/absence of genes within the operon as demonstrated by the two enterohemorrhagic strains (*E. coli* O26:H11 11368 and *E coli* O111:H1 11128, fig. 2). Given the

rapidity and complexity of gene degradation upon operon inactivation, it is not always possible to identify the event triggering the pseudogenization process. For instance, a large truncation does not preclude the pre-existence of a frameshift or of a nonsense mutation. Nevertheless, interesting patterns emerge from the comparison of different genomes. Namely, the presence of insertion sequences (ISs, 10 occurrences) and phage-related sequences (two occurrences) in the flanking regions of the *lsr* operon is only observed in genomes with an inactivated operon that are still in the process of pseudogenization, suggesting that these elements may be involved in rapid changes of gene content (supplementary table S1, Supplementary Material online). Among the 34 observed pseudogenes, 26 (76.5%) correspond to large truncations (>100 bp deletions), 6 (17.6%) to small indels (usually 1 or 2 bp insertions/deletions that cause disruption of the reading frame but also 7-bp deletion), and finally 2 (5.9%) were caused by single point mutations that lead to premature termination codon (supplementary table S1, Supplementary Material online).

We estimated the probability that the polymorphic pattern of presence/absence of the complete operon could have originated by neutral processes alone. To test this hypothesis, we generated 1,000 binary characters under a neutral process on the clade phylogeny and then determined the probability of obtaining the level of polymorphism observed in the data. We considered a model of evolution that assumes asymmetrical transition rates where the forward rate corresponds to the rate of gene inactivation and the backward rate corresponds to the rate of regaining a functional gene that was previously inactivated (see Materials and Methods). Among the many mechanisms that lead to gene inactivation, we considered point mutations, small insertions and deletions, large truncations, and IS transposition. To parameterize our model, we used published data. Single point mutations represented approximately 62.7% of the total mutational events causing gene inactivation in a recent large-scale experimental evolution experiment (Tenaillon et al. 2012). The mutation rate of *E. coli* was recently estimated to be $8.9 \times 10^{-11}$ per nucleotide per generation (Wielgoss et al. 2011). Together, these values lead to a rate of gene inactivation (forward rate) of approximately $1.17 \times 10^{-6}$ mutational events per generation for the *lsr* operon, considering that the total coding sequence is 8,271 bp.

The backward rate represents the rate of back mutation that overcomes single point mutations, the rate of insertion/deletion that reconstitutes a previous indel, the rate of excision of an IS, and the rate of gene conversion and lateral gene flow. The rate of back mutation will be negligible in relation to the rate of gene inactivation due to stop codons. The rate of excision of transposons is likely to be at least one order of magnitude smaller than the insertion rate (Charlesworth 1985). Lateral gene transfer probably occurs at a highly variable rate and is potentially the most important process that

can restore a functional operon. In the absence of estimations of these rates in natural setups, we tested multiple backward rates ranging four orders of magnitude (table 1). With all branches calibrated in units of generations (see Materials and Methods), we tested whether a neutral model could explain the data by contrasting the polymorphism level generated under neutrality and a similar model with rate parameters estimated from the data (forward rate = $6.89 \times 10^{-9}$, and backward rate = $4.00 \times 10^{-9}$). From all parameters tested, model 2x is the only model that generates a distribution of polymorphism with a median and a variance that includes the empirical level of polymorphism (0.38); however, this result implies a point mutation rate that is three orders of magnitude smaller than what was estimated empirically (Wielgoss et al. 2011). This is consistent with the interpretation that there is ongoing selection to maintain a functional operon in some strains of *E. coli*. Importantly, the level of polymorphism obtained by simulating 1,000 characters under a model with parameters estimated from the data is significantly different from the distribution generated with model 2x (forward = $1.17 \times 10^{-6}$, backward = $5.80 \times 10^{-7}$), mainly due to the large variance of the former (Kolmogorov–Smirnov text, $D = 0.2352$, $P$ value < 0.001, table 1).

## Phenotypic Characterization of Gene Losses

We made all single-gene deletions of the *lsr* operon as well as for two genes in the biosynthetic pathway of AI-2. We then determined the phenotypic effects for all deletions in terms of AI-2 accumulation and internalization in *E. coli* K-12 MG1655. AI-2 internalization profiles clearly show that every gene knockout leads to a measurable phenotypic effect, albeit some cause stronger phenotypic effects than others (fig. 3). In particular, mutants in the genes from the ABC transporter (*lsrB*, *lsrA*, *lsrC*, and *lsrD*) are less efficient in removing AI-2 from the extracellular medium, whereas the kinase mutant (*lsrK*) does not internalize the signal. The *lsrG* mutant, which is less efficient in degrading the inducer of the system (AI-2-P), and the repressor mutant (*lsrR*) are the only mutants that ensue a premature AI-2 internalization. These results are consistent with the previous studies on the characterization of the *lsr* operon and its regulation (Ren et al. 2004; Xavier and Bassler 2005a, 2005b; Li et al. 2007; Pereira et al. 2009), but here we show the phenotype of extracellular AI-2 accumulation for all the *lsr* single mutants. Our results show that extracellular AI-2 concentration is affected by every single-gene deletion. This can impact on how the different cells in the population sense the signal and therefore will impact on the selective pressure acting on each gene deletion.

Extrapolating the phenotypic effects of single knockout mutants obtained by genetic manipulation to the genotypes observed in the natural isolates suggests that gene deletions in natural strains decrease or abolish AI-2 internalization. The former corresponds to the two enterotoxigenic *E. coli* strains

**Table 1**

Distributions of Presence/Absence Polymorphism Generated under Diverse Evolutionary Models of Character Evolution

| | Forward Rate | Backward Rate | Ratio | Median | Variance | Kolmogorov–Smirnov Test |
|---|---|---|---|---|---|---|
| Empirical data | $6.89 \times 10^{-9}$ | $4.00 \times 10^{-9}$ | 1.72 | 0.356 | 0.0223 | — |
| Model 0.01x | $1.17 \times 10^{-6}$ | $1.17 \times 10^{-4}$ | 0.01 | 1.000 | 0.0002 | $D = 1, P < 0.001$ |
| Model 0.1x | $1.17 \times 10^{-6}$ | $1.17 \times 10^{-5}$ | 0.1 | 0.911 | 0.0019 | $D = 0.994, P < 0.001$ |
| Model 1x | $1.17 \times 10^{-6}$ | $1.17 \times 10^{-6}$ | 1 | 0.511 | 0.0057 | $D = 0.5245, P < 0.001$ |
| **Model 2x** | **$1.17 \times 10^{-6}$** | **$5.80 \times 10^{-7}$** | **2** | **0.333** | **0.0054** | **$D = 0.2352, P < 0.001$** |
| Model 5x | $1.17 \times 10^{-6}$ | $2.34 \times 10^{-7}$ | 5 | 0.178 | 0.0033 | $D = 0.6617, P < 0.001$ |
| Model 10x | $1.17 \times 10^{-6}$ | $1.17 \times 10^{-7}$ | 10 | 0.089 | 0.0021 | $D = 0.8498, P < 0.001$ |
| Model 100x | $1.17 \times 10^{-6}$ | $1.17 \times 10^{-8}$ | 100 | 0.000 | 0.0003 | $D = 0.987, P < 0.001$ |

NOTE.—Forward and backward rates are model parameters (see text), and the generated distributions are characterized by their median and variance of the relative frequency of strains with complete operon. These distributions were tested against the distribution generated with empirical parameters with a two-sample Kolmogorov–Smirnov test. The only model that generates a distribution of polymorphism that includes the empirical value (0.38) is in bold.
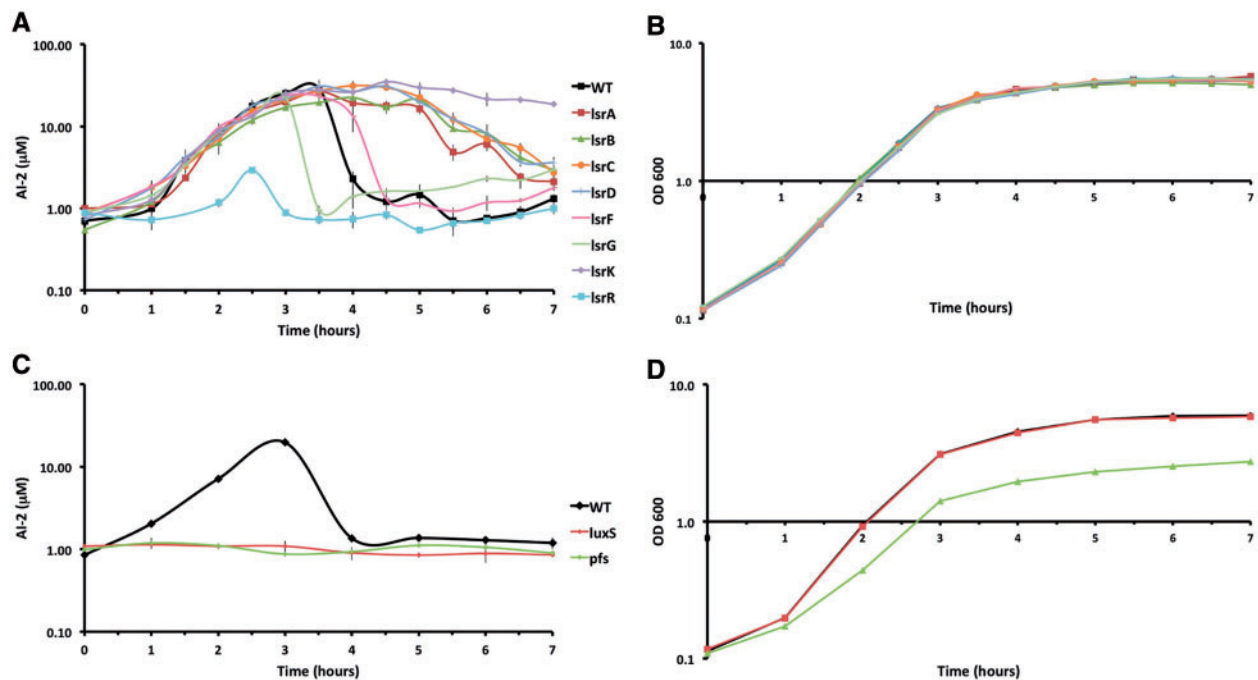


FIG. 3.—Extracellular AI-2 profiles of single-mutant knockouts cultured in LB at 37°C on the left, and respective absolute growth curves, on the right. On the top are results for single-gene knockout mutants of the *lsr* operon and below are results from knockout mutants of the genes involved in the AI-2 production pathway (*pfs* and *luxS*). WT, wild type.

(*E. coli* O139:H28 E24377A and *E. coli* UMNK88). These strains have an impaired Lsr transporter, but due to the presence of functional kinase and repressor, it is expected that these strains are still capable of internalizing the signal, albeit at a lower rate via a less efficient system (Pereira et al. 2012). On the other hand, all other natural strains without a complete *lsr* operon lack a functional *lsrK*, which is sufficient to prevent any decrease of the extracellular AI-2 concentration. LsrK is responsible for producing the inducer of the system (AI-2-P) and in its absence, even if the receptor gene (*lsrB*) is present, the protein is not expressed, hence *lsrK* mutants are impaired not only in AI-2 internalization but also in AI-2 sensing. The loss of *lsrR* leads to a constitutive expression

of the *lsr* operon and thus to a very low accumulation of AI-2 in the extracellular medium because all AI-2 that is produced is also internalized. Interestingly, the *lsrR* gene is only absent in the genomes that also lack a functional ABC transporter (LsrACDB) and the corresponding signal kinase (LsrK). Therefore, also in these genomes, we would predict an overall phenotypic effect that is similar to a complete absence of the *lsr* operon and to no internalization of AI-2 by those cells. Hence, we do not expect a more efficient removal of the AI-2 signal from the extracellular medium for any of the natural isolates analyzed.

Interestingly, in monocultures, and under the experimental conditions tested, the *luxS* and all *lsr* mutants show small, if

any, differences in growth rates (fig. 3). This suggests a weak metabolic fitness cost for the QS and contrasts with a deletion in the *pfs* gene, the enzyme upstream of *luxS* responsible for the degradation of SAH (fig. 1) that carries major fitness costs to the cell (fig. 3). This is important given that both *pfs* and *luxS* mutants have the same key effect of not producing AI-2 (flat curves of fig. 3C).

### Genetic Diversity and Levels of Selection

Pairwise nucleotide diversity (π) varies across the genes in the operon (fig. 4 and table 2). It is particularly high in the *lsrA* gene encoding the ABC-ATPase enzyme that provides the energy necessary for the internalization of AI-2 into the cell, and in its two flanking genes *lsrR* and *lsrC*, but in every case, the levels of diversity are within the range of those observed in the core genome, even when controlling for similar codon usage bias (fig. 4). The level of diversity for nonsynonymous substitutions is much lower than for synonymous in all genes, consistent with some degree of evolutionary constrain (table 2). This is corroborated by the pattern of intermediate levels of codon usage bias recovered from the several measures used (table 2).

Nonsynonymous substitution patterns are not significantly different between complete genes in functional operons and complete genes in partly inactivated operons as would be expected for genes under relaxed purifying selection (fig. 4). This suggests that either the cell is still using these genes or that the process of pseudogenization is too recent to have left a signature in the patterns of substitution. The gene *lsrG*, which encodes one of the two enzymes responsible for processing of

AI-2-P, is an exception as it shows high nucleotide diversity caused by an increased number of nonsynonymous substitutions (fig. 4, white triangles). This gene seems to be always the last to pseudogenize and hence would have more time to accumulate changes.

To test for signatures of selection on shaping levels and patterns of diversity, we performed McDonald–Kreitman and Tajima's *D* tests (table 3). Tajima's *D* statistic was not significantly different from zero in any of the genes analyzed. Tajima's *D* is highly sensitive to population demography (Simonsen et al. 1995), and it tends to assume negative values in expanding populations. Because it was proposed that *E. coli* population enjoyed a large recent population expansion (Wirth et al. 2006), expected value of *D* is negative (and not zero) based on demographic effects. We then decided to use McDonald–Kreitman tests to analyze the patterns of selection in this work because this test is much more robust to demographic effects (Nielsen 2005). Both LuxS (AI-2 synthase) and LsrA have a pattern of diversity that rejects the null model of neutrality (McDonald–Kreitman test, table 3) but for very different reasons. The gene *luxS* shows levels of nonsynonymous polymorphism close to the average gene but much smaller nonsynonymous divergence (after normalization by synonymous substitutions, fig. 5). This is suggestive of strong purifying selection on nonsynonymous polymorphisms. On the other hand, nonsynonymous polymorphisms are much more abundant in *lsrA* than in all the others genes after normalization by synonymous rates (PS and DS). The pattern for *lsrA* suggests the maintenance of high nonsynonymous polymorphism segregating in the population.
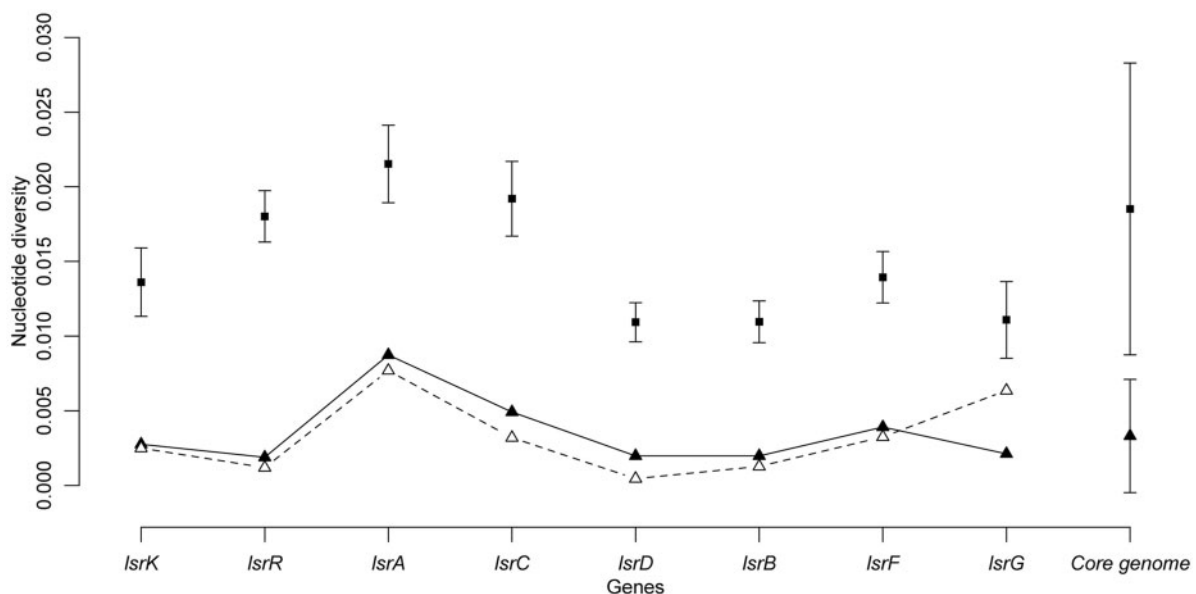


Fɪɢ. 4.—Genetic diversity at the *lsr* operon. Black squares indicate total nucleotide diversity (mean and standard deviation) for each gene in the operon. Triangles are nucleotide diversity at nonsynonymous sites estimated in complete genes for strains with the full *lsr* operon (black) and for strains with partial *lsr* operons (white). For comparison, the total nucleotide diversity and nonsynonymous diversity of core genes with similar codon usage was added.

**Table 2**

Genetic Diversity and Codon Usage

| | Gene | $L$ | $S$ | $N$ | $h$ | $\pi_{total}$ Mean | $\pi_{total}$ SD | $\pi_S$ | $\pi_{NS}$ | No. of Codons | ENC | CBI | CAI | eCAI | CAI/eCAI |
|---|---|---|---|---|---|---|---|---|---|---|---|---|---|---|---|
| Strains with complete *lsr* operon | *lsrK* | 1,593 | 85 | 15 | 10 | 0.014 | 0.0023 | 0.047 | 0.003 | 530 | 51.728 | 0.325 | 0.315 | 0.337 | 0.935 |
| | *lsrR* | 954 | 58 | 15 | 9 | 0.018 | 0.0017 | 0.067 | 0.002 | 317 | 53.143 | 0.375 | 0.302 | 0.325 | 0.929 |
| | *lsrA* | 1,533 | 116 | 15 | 12 | 0.022 | 0.0026 | 0.059 | 0.009 | 511 | 46.361 | 0.433 | 0.322 | 0.328 | 0.982 |
| | *lsrC* | 1,029 | 74 | 15 | 11 | 0.019 | 0.0025 | 0.058 | 0.005 | 342 | 48.842 | 0.440 | 0.333 | 0.310 | 1.075 |
| | *lsrD* | 993 | 35 | 15 | 11 | 0.011 | 0.0013 | 0.035 | 0.002 | 330 | 45.614 | 0.433 | 0.295 | 0.302 | 0.976 |
| | *lsrB* | 1,023 | 40 | 15 | 12 | 0.011 | 0.0014 | 0.040 | 0.002 | 340 | 49.022 | 0.331 | 0.363 | 0.349 | 1.040 |
| | *lsrF* | 876 | 47 | 15 | 12 | 0.014 | 0.0017 | 0.047 | 0.004 | 291 | 44.400 | 0.518 | 0.344 | 0.343 | 1.003 |
| | *lsrG* | 291 | 15 | 15 | 8 | 0.011 | 0.0026 | 0.043 | 0.002 | 96 | 48.112 | 0.504 | 0.489 | 0.398 | 1.228 |
| All strains | *luxS* | 516 | 21 | 40 | 20 | 0.010 | 0.0005 | 0.029 | 0.003 | 171 | 45.907 | 0.517 | 0.497 | 0.366 | 1.359 |

Note.—*L* is sequence length, *s* is the number of segregating sites, *N* is sample size, and *h* is the number of unique haplotypes, and π is nucleotide diversity (mean and standard deviation). Nucleotide diversity is presented for total sequence, synonymous sites (S), and nonsynonymous sites (NS) only. ENC is the effective number of codons, CBI is the Codon Bias Index, CAI is the Codon Adaptation Index, and eCAI is the effective number of codons. Genes in the *lsr* operon are ordered following position on the chromosome.

**Table 3**

Neutrality Tests

| | | Tajima's $D$ | McDonald and Kreitman test | | | | | | | DOS |
|---|---|---|---|---|---|---|---|---|---|---|
| | | | $D_N$ | $D_S$ | $P_N$ | $P_S$ | $P$ | $\alpha$ | NI | |
| Strains with complete *lsr* operon | *lsrK* | −0.7462 | 9 | 80 | 14 | 71 | 0.265 | −0.753 | 1.753 | −0.064 |
| | *lsrR* | −0.2277 | 3 | 23 | 6 | 53 | 1.000 | 0.132 | 0.868 | 0.014 |
| | *lsrA* | −0.5846 | 11 | 84 | 34 | 87 | 0.004** | −1.984 | 2.984 | −0.165 |
| | *lsrC* | −0.6240 | 4 | 36 | 15 | 60 | 0.198 | −1.250 | 2.250 | −0.100 |
| | *lsrD* | 0.0367 | 5 | 41 | 4 | 31 | 1.000 | −0.058 | 1.058 | −0.006 |
| | *lsrB* | −0.4743 | 6 | 28 | 9 | 32 | 0.775 | −0.313 | 1.313 | −0.043 |
| | *lsrF* | −0.7434 | 1 | 8 | 12 | 36 | 0.668 | −1.667 | 2.667 | −0.139 |
| | *lsrG* | −1.3815 | 0 | 2 | 2 | 14 | 1.000 | — | — | −0.125 |
| All strains | *luxS* | −0.1734 | 0 | 14 | 7 | 15 | 0.029* | — | — | −0.318 |

Note.—$D_S$ and $D_N$ are fixed synonymous and nonsynonymous substitutions, $P_S$ and $P_N$ are segregating synonymous and nonsynonymous substitutions. *P* value (two tailed) is the significant level of the Fisher exact test that $D_N/D_S = P_N/P_S$. $\alpha = 1 - NI$, and NI is the neutrality index, $\alpha$ is the proportion of evolutionary change that is due to positive selection, these values cannot be computed when $D_N$ is zero. DOS is direction of selection. Divergence was estimated between *E. coli* strains against the closest outgroup (*E. fergusonii*).

The patterns of high dN/dS between closely related strains for *lsrA* might arise simply from the presence of newly created slightly deleterious mutations that have not yet had time to be purged (Rocha et al. 2006). However, the high effective population size of *E. coli* should lead to a rapid elimination of these mutations. Indeed, we found that dN/dS falls rapidly to low values in the core genome (supplementary fig. S3, Supplementary Material online). When we compare the average trend of dN/dS over patristic distances with that of *lsrA,* we find much higher values for the latter, suggesting that slow purifying selection of slightly deleterious changes is not driving the differences between the two sets. This trend could result from a lower number of deleterious nonsynonymous changes in this gene relative to the core. However, when we compared *E. coli* with *E. fergusonii,* there was no difference in dN/dS between *lsrA* and the core genome. The observation of an excess of dN/dS in *lsrA* relative to core genome within the species and identical dN/dS in the two sets when comparisons

are made between species fits very well the hypothesis of diversifying selection for *lsrA*.

Figure 6 shows for *lsrA* and for *luxS* a sliding window analysis of the ratio of nonsynonymous to synonymous substitutions segregating within *E. coli* and between *E. coli* and *E. fergusonii*. The asterisks indicate the approximate gene location of codons where a significant signal of selection was detected with the codon-based approach. Three significant codons distributed throughout the gene (positions 76, 181, and 482) were detected for *lsrA*, whereas only one codon (position 145) was identified for *luxS*.

## Discussion

We have found that *E. coli* exhibits a gene repertoire polymorphism in the *lsr* operon. We have experimentally shown that such polymorphism leads to cells lacking the ability to bind, internalize, and/or process the QS signal. However, all
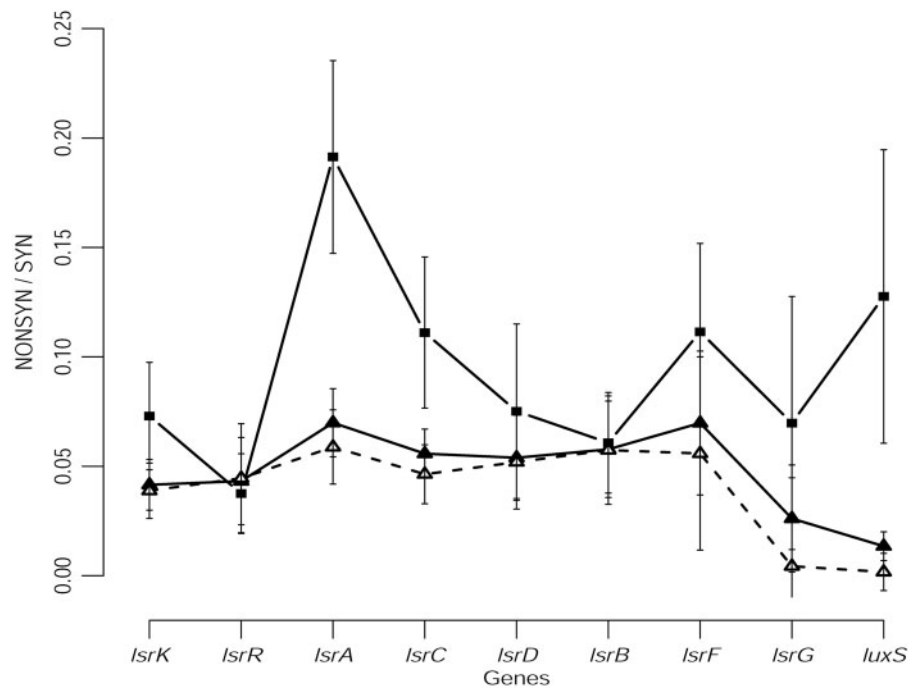
FIG. 5.—Nonsynonymous to synonymous rates across genes in the *lsr* operon and the *luxS*. Intraspecific comparisons correspond to nucleotide diversity for synonymous and nonsynonymous sites (black squares), whereas comparisons with the outgroup (*Escherichia fergusonii*) correspond to synonymous and nonsynonymous nucleotide divergence (triangles). Black triangles are average nucleotide differences between species, whereas white triangles correspond to net divergence, which subtracts to the previous statistic the average nucleotide differences for polymorphic sites. Error bars are standard errors estimated after 1,000 bootstrap replicates.

strains maintain a functional LuxS, the synthase of the QS signal, even though the fitness cost of this deletion in monocultures is as low as that of many *lsr* genes. Overall, the evolution of the genes essential for regulating AI-2 concentration was shown here to be complex and non-neutral. Fifty-eight percent of *E. coli* strains cannot regulate AI-2 extracellular concentrations, 23 of the 40 strains analyzed lack a functional LsrK, these strains produce AI-2 but do not have the ability to sense or remove AI-2 from itself or others. We did not find any natural strain that lacks the LsrR repressor and still have a potentially functional operon. This suggests counter selection of strains that could be more efficient at removing AI-2. Hence, the overall phenotypic effect of the observed operon pseudogenization is always toward the decrease or total abolishment of AI-2 internalization and removal from the environment. Importantly, the comparative genomic analyses indicate that this functional polymorphism is maintained by natural selection.

We find both signatures of selection to lose the operon and selection to maintain it, creating a balanced polymorphism at the level of gene content. This leads to a frequency of the *lsr* operon intermediate between that of persistent and of volatile genes (van Passel et al. 2008; Kuo and Ochman 2009; Touchon et al. 2009) The selective pressure to lose the operon is supported by the inference of at least eight independent events of operon inactivation and the observation

that pseudogenization, when it occurs, is too fast to be a neutral process. This fast gene extinction dynamics was already observed in the genomes of *Salmonella enterica* vs. Gallinarum (Kuo and Ochman 2010) and occurs through the same general mechanisms described for bacterial pseudogene formation (e.g., large truncations, small frameshift indels, and stop codons) (Lerat and Ochman 2005; Ochman and Davalos 2006). Although our data differ from Kuo and Ochman (2010) in that all genes are inferred to be ancestral and pseudogenization is shared with many strains, some of which very distantly related. In that study, the authors analyze 147 pseudogenes of which only five were shared with the closest related strain and only three are inferred to be ancestral. Our data fit better the models of balancing selection than a random model of gene loss, even though we cannot exclude the possibility that pseudogenization of one gene accelerates the loss of the other genes in the operon. Selection to maintain the ability to respond to extracellular AI-2 is suggested by balancing selection patterns in *lsrA* gene, as well as the polymorphism observed in all other *lsr* genes of complete operons that are typical of functional genes. In addition, we inferred through simulation that the majority of the *E. coli* strains should have already lost the operon unless there is ongoing selective pressure to maintain it.

The mechanisms of selection maintaining these polymorphisms are an important line of future research. Theoretical
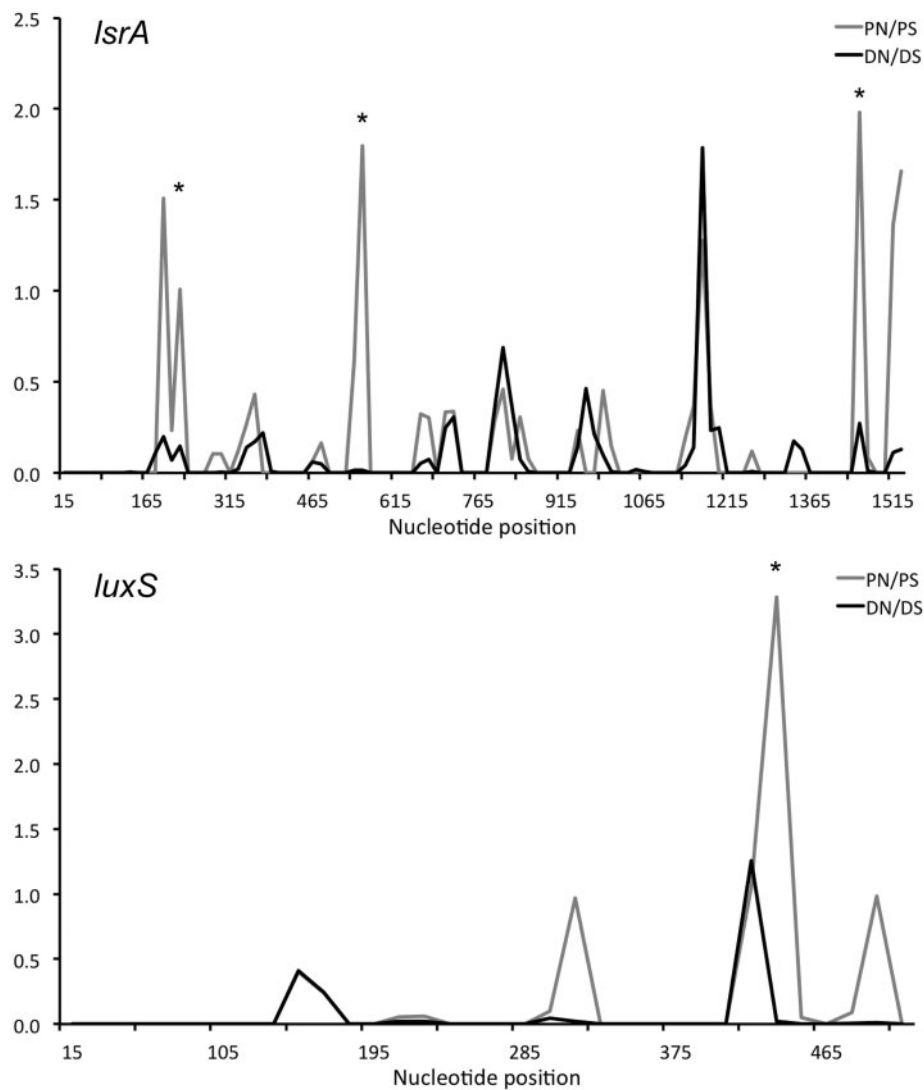
**FIG. 6.**—Sliding window analysis of the ratio of nonsynonymous (N) to synonymous (S) substitutions segregating within *Escherichia coli* (P) and between *E. coli* and *E. fergusonii* (D) across *lsrA* and *luxS* genes. Window size is 30 bp with 15-bp steps. Sample size is 15 for *lsrA* and 40 for *luxS* corresponding to strains with complete operons and all natural strains, respectively. Asterisks indicate approximate position of codons identified as targets of selection (codons 76, 181, and 482 in LsrA, and codon 145 in LuxS).

models have shown that balancing selection may occur for diverse reasons and could potentially be quite common (Gillespie 2004). We propose two nonmutually exclusive hypotheses for the maintenance of polymorphisms in this system. We observed that all *Shigella* and AIEC, which are strains known to replicate within macrophages, lack the *lsr* operon. The loss of the *lsr* operon in these strains could thus be a consequence of adaptation to a specific pathovar. This fits the hypothesis that cooperative processes regulated by QS are less important in bacteria with low infectious dose and able to replicate in professional phagocytes (Gama et al. 2012). However, this intracellular niche adaptation hypothesis cannot explain all losses observed in our data because many other strains lack *lsr*.

The other hypothesis relates to the social consequences of mutations in the genes regulating AI-2 QS. We found no measurable growth cost for the loss of AI-2 QS mechanism (fig. 3), but in *E. coli,* AI-2 regulates costly group behaviors such as virulence and biofilm formation (González-Barrios et al. 2006; Herzberg et al. 2006; Reisner et al. 2006; Zhu et al. 2007; Lee et al. 2011). Hence, although QS mutations have little direct metabolic effects, as growth is not affected in monocultures, they are likely to have ecological benefits by providing the cells the ability to exploit social processes in microbiomes. In most QS systems of Gram-negative bacteria, high cell densities are associated with high concentration of the signal. Elements that have lost the ability of producing the signal but still benefit from the information of producers

(emitters) are thus noncooperating and have a fitness advantage (Diggle et al. 2007), in these systems receptors are much more abundant than emitters (Patankar and González 2009). In contrast, in the *E. coli* AI-2 QS system, we observed gene repertoire polymorphism at the level of the signal receptor (*lsr* operon) and not at the signal emitter (*luxS*). All these gene losses reduce or abolish AI-2 reception and internalization but do not reduce AI-2 production. This can be interpreted as coercive behavior, which is a particular type of social cheating if demonstrated that these cells would benefit from forcing the nearby cells into cooperative behaviors, while themselves refraining from cooperating (Diggle et al. 2007; Foster et al. 2007). Consistently, it was shown that *E. coli lsr* mutants can induce the onset of cooperative behaviors of *Vibrio harveyi* and *V. cholerae* even when they are at low quorum (Xavier and Bassler 2005a)

Because AI-2 has been shown to regulate biofilm formation and virulence traits in *E. coli*, it is expectable that the cells that do not internalize AI-2 but still contribute to their increased concentration in the extracellular medium will promote the remaining AI-2-sensitive cells in the vicinity to hasten the onset of the behavior they regulate with AI-2. It was recently predicted by Van Dyken and Wade (2012) that when social cheaters are maintained in natural populations as an evolutionary stable strategy, then it should also be expected that cheaters would be characterized by large insertion/deletions, frameshift mutations, or premature STOP codons; these are features that characterize the *lsr* operons of *E. coli* natural variants that do not regulate extracellular AI-2.

The interpretation that gene repertoire polymorphism in the *lsr* operon is maintained through a process of social evolution is further strengthened by the observation that *luxS*, the signal synthase, is present in all strains (fig. 2) even though we detect no fitness effect in the single-gene knockout mutant monocultures (fig. 3). Because of its enzymatic role in recycling products of SAM metabolism, it was suggested that the selective pressure to maintain *luxS* was primarily to detoxify the cell and recycle the products of SAM metabolism (Schauder et al. 2001; Winzer et al. 2003; Vendeville et al. 2005; De Keersmaecker et al. 2006; Hardie and Heurlier 2008). Importantly, we show that a mutant in Pfs, the enzyme immediately upstream of LuxS in the metabolism of SAM, does show a marked growth defect (fig. 3) probably due to the toxic accumulation of SAH (Schauder et al. 2001; Winzer et al. 2002). This strongly indicates that Pfs, not LuxS, is the major enzyme responsible for preventing the toxic consequences of SAH accumulation. The similarity in the phenotypic effects and their extreme difference in fitness cost highlight the importance of *pfs* in central metabolism, and it suggests that the selective pressure to maintain a functional *luxS* in the cell is not metabolic but social. Naturally, this conclusion has to be contextualized in the whole discussion of the AI-2 as a QS signal; a social cost cannot be attributed to any gene that does not present a strong metabolic cost.

We still lack a direct experimental demonstration of such social benefit. This is difficult to show for inter-specific QS because it requires experimentation in complex environments. Nevertheless, it is known that in the vertebrate gut, *E. coli* experiences a complex multispecies environment where the ability to interact (or interfere) with other cells, of the same or of different species, may influence the evolution of its AI-2 regulation system (McNab et al. 2003). Interestingly, extraintestinal virulence of an *E. coli* AI-2 QS-negative strain (*E. coli* B2S) was shown to be boosted in mix strains infections compared with pure culture infections when mixed with an AI-2 QS positive regarded as commensal (*E. coli* MG1655) (Tourret et al. 2011). Hence, QS polymorphisms might lead to exploitation of commensals by pathogens to increase virulence.

Overall, our findings suggest that complex adaptations of species with polyclonal interactions, such as *E. coli*, can be due to genes maintained at intermediary frequencies rather than ubiquitous or pathovar-specific genes.

## Supplementary Material

Supplementary tables S1 and S2 and figures S1–S3 are available at *Genome Biology and Evolution* online (http://gbe.oxfordjournals.org/).

## Acknowledgments

## Literature Cited

Baba T, et al. 2006. Construction of *Escherichia coli* K-12 in-frame, single-gene knockout mutants: the Keio collection. Mol Syst Biol. 2: 2006.0008.

Bansal T, Jesudhasan P, Pillai S, Wood TK, Jayaraman A. 2008. Temporal regulation of enterohemorrhagic *Escherichia coli* virulence mediated by autoinducer-2. Appl Microbiol Biotechnol. 78:811–819.

Blattner FR, et al. 1997. The complete genome sequence of *Escherichia coli* K-12. Science 277:1453–1462.

Charlesworth B. 1985. The population genetics of transposable elements. In: Ohta T, Aoki K, editors. Population genetics and molecular evolution. Berlin (Germany): Springer-Verlag. p. 213–232.

Chen X, et al. 2002. Structural identification of a bacterial quorum-sensing signal containing boron. Nature 415:545–549.

Clemente JC, Ursell LK, Parfrey LW, Knight R. 2012. The impact of the gut microbiota on human health: an integrative view. Cell 148:1258–1270.

Crespi BJ. 2001. The evolution of social behavior in microorganisms. Trends Ecol Evol. 16:178–183.

De Keersmaecker SCJ, Sonck K, Vanderleyden J. 2006. Let LuxS speak up in AI-2 signaling. Trends Microbiol. 14:114–119.

Diggle SP, Gardner A, West SA, Griffin AS. 2007. Evolutionary theory of bacterial quorum sensing: when is a signal not a signal? Philos Trans R Soc Lond B Biol Sci. 362:1241–1249.

Edgar RC. 2004. MUSCLE: multiple sequence alignment with high accuracy and high throughput. Nucleic Acids Res. 32:1792–1797.

Escobar-Páramo PP, Giudicelli CC, Parsot CC, Denamur EE. 2003. The evolutionary history of *Shigella* and enteroinvasive *Escherichia coli* revised. J Mol Evol. 57:140–148.

Foster KR, Parkinson K, Thompson CRL. 2007. What can microbial genetics teach sociobiology? Trends Genet. 23:74–80.

Gama JA, Abby SS, Vieira-Silva S, Dionisio F, Rocha EPC. 2012. Immune subversion and quorum-sensing shape the variation in infectious dose among bacterial pathogens. PLoS Pathog. 8:e1002503.

Garrett WS, Gordon JI, Glimcher LH. 2010. Homeostasis and inflammation in the intestine. Cell 140:859–870.

Gascuel O. 1997. BIONJ: an improved version of the NJ algorithm based on a simple model of sequence data. Mol Biol Evol. 14:685–695.

Gillespie JH. 2004. Population genetics: a concise guide, 2nd ed. Baltimore (MD): Johns Hopkins University Press.

Glasser AL, et al. 2001. Adherent invasive *Escherichia coli* strains from patients with Crohn's disease survive and replicate within macrophages without inducing host cell death. Infect Immun. 69:5529–5537.

González-Barrios AF, et al. 2006. Autoinducer 2 controls biofilm formation in *Escherichia coli* through a novel motility quorum-sensing regulator (MqsR, B3022). J Bacteriol. 188:305–316.

Hardie K, Heurlier K. 2008. Establishing bacterial communities by "word of mouth": LuxS and autoinducer 2 in biofilm development. Nat Rev Microbiol. 6:635–643.

Hegde M, et al. 2011. Chemotaxis to the quorum-sensing signal AI-2 requires the Tsr chemoreceptor and the periplasmic LsrB AI-2-binding protein. J Bacteriol. 193:768–773.

Herzberg M, Kaye IK, Peti W, Wood TK. 2006. YdgG (TqsA) controls biofilm formation in *Escherichia coli* K-12 through autoinducer 2 transport. J Bacteriol. 188:587–598.

Hudson RR. 1990. Gene genealogies and the coalescent process. In: Futuyma D, Antonovics J, editors. Oxford surveys in evolutionary biology, Vol. 7. Oxford (UK): Oxford University Press. p. 1–44.

Kaper JB, Nataro JP, Mobley HLT. 2004. Pathogenic *Escherichia coli*. Nat Rev Microbiol. 2:123–140.

Keller L, Surette MG. 2006. Communication in bacteria: an ecological and evolutionary perspective. Nat Rev Microbiol. 4:249–258.

Kosakovsky Pond SL, Frost SDW. 2005. Datamonkey: rapid detection of selective pressure on individual sites of codon alignments. Bioinformatics 21:2531–2533.

Kosakovsky Pond SL, et al. 2006. Adaptation to different human populations by HIV-1 revealed by codon-based analyses. PLoS Comp Biol. 2:e62.

Kuo C-H, Ochman H. 2009. The fate of new bacterial genes. FEMS Microbiol Rev. 33:38–43.

Kuo C-H, Ochman H. 2010. The extinction dynamics of bacterial pseudogenes. PLoS Genet. 6:e1001050.

Lawrence JG, Ochman H, Hartl DL. 1991. Molecular and evolutionary relationships among enteric bacteria. J Gen Microbiol. 137:1911–1921.

Lee J-HJ, Kim Y-GY, Cho MHM, Wood TKT, Lee JJ. 2011. Transcriptomic analysis for genetic mechanisms of the factors related to biofilm formation in *Escherichia coli* O157:H7. Curr Microbiol. 62:1321–1330.

Lerat E, Ochman H. 2005. Recognizing the pseudogenes in bacterial genomes. Nucleic Acids Res. 33:3125–3132.

Li J, et al. 2007. Quorum sensing in *Escherichia coli* is signaled by AI-2/LsrR: effects on small RNA and biofilm architecture. J Bacteriol. 189:6011–6020.

Librado P, Rozas J. 2009. DnaSP v5: a software for comprehensive analysis of DNA polymorphism data. Bioinformatics 25:1451–1452.

Luo C, et al. 2011. Genome sequencing of environmental *Escherichia coli* expands understanding of the ecology and speciation of the model bacterial species. Proc Natl Acad Sci U S A. 108:7200–7205.

Maddison WP, Maddison DR. 2011. Mesquite: a modular system for evolutionary analysis. Version 2.75. Available from: http://mesquiteproject.org (last accessed January 2, 2013).

McDonald J, Kreitman M. 1991. Adaptive protein evolution at the Adh locus in *Drosophila*. Nature 351:652–654.

McNab R, et al. 2003. LuxS-based signaling in *Streptococcus gordonii*: autoinducer 2 controls carbohydrate metabolism and biofilm formation with *Porphyromonas gingivalis*. J Bacteriol. 185:274–284.

Moreno E, et al. 2009. Structure and urovirulence characteristics of the fecal *Escherichia coli* population among healthy women. Microbes Infect. 11:274–280.

Morton BRB. 1993. Chloroplast DNA codon use: evidence for selection at the psb A locus based on tRNA availability. J Mol Evol. 37:273–280.

Nielsen R. 2005. Molecular signatures of natural selection. Annu Rev Genet. 39:197–218.

Nowrouzian FL, Wold AE, Adlerberth I. 2005. *Escherichia coli* strains belonging to phylogenetic group B2 have superior capacity to persist in the intestinal microflora of infants. J Infect Dis. 191:1078–1083.

Ochman H, Davalos L. 2006. The nature and dynamics of bacterial genomes. Science 311:1730–1733.

Ochman H, Whittam TS, Caugant DA, Selander RK. 1983. Enzyme polymorphism and genetic population structure in *Escherichia coli* and *Shigella*. J Gen Microbiol. 129:2715–2726.

Oh SS, Buddenborg SS, Yoder-Himes DRD, Tiedje JMJ, Konstantinidis KTK. 2012. Genomic diversity of *Escherichia* isolates from diverse habitats. PLoS One 7:e47005–e47005.

Pagel M. 1994. Detecting correlated evolution on phylogenies: a general method for the comparative analysis of discrete characters. Proc R Soc Lond B Biol Sci. 255:37–45.

Patankar AV, González JE. 2009. Orphan LuxR regulators of quorum sensing. FEMS Microbiol Rev. 33:739–756.

Pereira CS, de Regt AK, Brito PH, Miller ST, Xavier KB. 2009. Identification of functional LsrB-like autoinducer-2 receptors. J Bacteriol. 191:6975–6987.

Pereira CS, McAuley JR, Taga ME, Xavier KB, Miller ST. 2008. *Sinorhizobium meliloti*, a bacterium lacking the autoinducer-2 (AI-2) synthase, responds to AI-2 supplied by other bacteria. Mol Microbiol. 70:1223–1235.

Pereira CS, Thompson JA, Xavier KB. Forthcoming 2012. AI-2-mediated signalling in bacteria. FEMS Microbiol Rev.

Pereira CS, et al. 2012. Phosphoenolpyruvate phosphotransferase system regulates detection and processing of the quorum sensing signal autoinducer-2. Mol Microbiol. 84:93–104.

Pond SLK, Frost SDW. 2005. Not so different after all: a comparison of methods for detecting amino acid sites under selection. Mol Biol Evol. 22:1208–1222.

Puigbò P, Bravo IG, Garcia-Vallvé S. 2008. E-CAI: a novel server to estimate an expected value of Codon Adaptation Index (eCAI). BMC Bioinformatics 9:65.

Pupo GMG, Lan RR, Reeves PRP. 2000. Multiple independent origins of *Shigella* clones of *Escherichia coli* and convergent evolution of many of their characteristics. Proc Natl Acad Sci U S A. 97: 10567–10572.

Reisner A, Krogfelt KA, Klein BM, Zechner EL, Molin S. 2006. In vitro biofilm formation of commensal and pathogenic *Escherichia coli* strains: impact of environmental and genetic factors. J Bacteriol. 188:3572–3581.

Ren D, Bedzyk L, Ye R, Thomas S, Wood T. 2004. Stationary-phase quorum-sensing signals affect autoinducer-2 and gene expression in *Escherichia coli*. Appl Environ Microbiol. 70:2038–2043.

Rocha EPC, Touchon M, Feil EJ. 2006. Similar compositional biases are caused by very different mutational effects. Genome Res. 16: 1537–1547.

Rocha EPC, et al. 2006. Comparisons of dN/dS are time dependent for closely related bacterial genomes. J Theor Biol. 239:226–235.

Schauder S, Shokat K, Surette MG, Bassler BL. 2001. The LuxS family of bacterial autoinducers: biosynthesis of a novel quorum-sensing signal molecule. Mol Microbiol. 41:463–476.

Schluter D, Price T, Mooers A, Ludwig D. 1997. Likelihood of ancestor states in adaptive radiation. Evolution 51:1699–1711.

Schmidt HA, Strimmer K, Vingron M, Haeseler von A. 2002. TREE-PUZZLE: maximum likelihood phylogenetic analysis using quartets and parallel computing. Bioinformatics 18:502–504.

Sharp PM, Li WH. 1986. Codon usage in regulatory genes in *Escherichia coli* does not reflect selection for "rare" codons. Nucleic Acids Res. 14: 7737–7749.

Sharp PM, Li WH. 1987. The Codon Adaptation Index—a measure of directional synonymous codon usage bias, and its potential applications. Nucleic Acids Res. 15:1281–1295.

Silhavy TJ, Berman ML, Enquist LW. 1984. Experiments with gene fusions. New York: Cold Spring Harbor Press.

Simonsen KL, Churchill GA, Aquadro CF. 1995. Properties of statistical tests of neutrality for DNA polymorphism data. Genetics 141:413–429.

Stoletzki N, Eyre-Walker A. 2011. Estimation of the neutrality index. Mol Biol Evol. 28:63–70.

Surette MG, Miller MB, Bassler BL. 1999. Quorum sensing in *Escherichia coli*, *Salmonella typhimurium*, and *Vibrio harveyi*: a new family of genes responsible for autoinducer production. Proc Natl Acad Sci U S A. 96:1639–1644.

Taga ME, Xavier KB. 2011. Methods for analysis of bacterial autoinducer-2 production. Curr Protoc Microbiol. Chapter 1:Unit1C.1.

Tajima F. 1989. Statistical method for testing the neutral mutation hypothesis by DNA polymorphism. Genetics 123:585–595.

Tamura KK, Dudley JJ, Nei MM, Kumar SS. 2007. MEGA4: molecular evolutionary genetics analysis (MEGA) software version 4.0. Mol Biol Evol. 24:1596–1599.

Tenaillon O, Skurnik D, Picard B, Denamur E. 2010. The population genetics of commensal *Escherichia coli*. Nat Rev Microbiol. 8:207–217.

Tenaillon O, et al. 2012. The molecular diversity of adaptive convergence. Science 335:457–461.

Touchon M, et al. 2009. Organised genome dynamics in the *Escherichia coli* species results in highly diverse adaptive paths. PLoS Genet. 5: e1000344.

Tourret J, et al. 2011. The interaction between a non-pathogenic and a pathogenic strain synergistically enhances extra-intestinal virulence in *Escherichia coli*. Microbiology 157:774–785.

Van Dyken JD, Wade MJ. 2012. Detecting the molecular signature of social conflict: theory and a test with bacterial quorum sensing genes. Am Nat. 179:436–450.

van Passel MWJ, Marri PR, Ochman H. 2008. The emergence and fate of horizontally acquired genes in *Escherichia coli*. PLoS Comp Biol. 4: e1000059.

Vendeville A, Winzer K, Heurlier K, Tang CM, Hardie KR. 2005. Making "sense" of metabolism: autoinducer-2, LUXS and pathogenic bacteria. Nat Rev Microbiol. 3:383–396.

Wang L, Hashimoto Y, Tsao C-Y, Valdes JJ, Bentley WE. 2005. Cyclic AMP (cAMP) and cAMP receptor protein influence both synthesis and uptake of extracellular autoinducer 2 in *Escherichia coli*. J Bacteriol. 187:2066–2076.

Wang L, Li J, March JC, Valdes JJ, Bentley WE. 2005. luxS-dependent gene regulation in *Escherichia coli* K-12 revealed by genomic expression profiling. J Bacteriol. 187:8350–8360.

Waters CM, Bassler BL. 2005. Quorum sensing: cell-to-cell communication in bacteria. Annu Rev Cell Dev Biol. 21:319–346.

West SA, Diggle SP, Buckling A, Gardner A, Griffins AS. 2007. The social lives of microbes. Annu Rev Ecol Evol S. 38:53–77.

West SA, Griffin AS, Gardner A, Diggle SP. 2006. Social evolution theory for microorganisms. Nat Rev Microbiol. 4:597–607.

Wielgoss S, et al. 2011. Mutation rate inferred from synonymous substitutions in a long-term evolution experiment with *Escherichia coli*. G3. Genes Genomes Genet. 1:183–186.

Winzer K, Hardie KR, Williams P. 2002. Bacterial cell-to-cell communication: sorry, can't talk now—gone to lunch! Curr Opin Microbiol. 5: 216–222.

Winzer K, Hardie KR, Williams P. 2003. LuxS and autoinducer-2: their contribution to quorum sensing and metabolism in bacteria. Adv Appl Microbiol. 53:291–396.

Winzer K, et al. 2002. LuxS: its role in central metabolism and the in vitro synthesis of 4-hydroxy-5-methyl-3(2H)-furanone. Microbiology 148: 909–922.

Wirth T, et al. 2006. Sex and virulence in *Escherichia coli*: an evolutionary perspective. Mol Microbiol. 60:1136–1151.

Wold AEA, Caugant DAD, Lidin-Janson GG, de Man PP, Svanborg CC. 1992. Resident colonic *Escherichia coli* strains frequently display uropathogenic characteristics. J Infect Dis. 165:46–52.

Wright F. 1990. The "effective number of codons" used in a gene. Gene 87:23–29.

Xavier KB, Bassler BL. 2003. LuxS quorum sensing: more than just a numbers game. Curr Opin Microbiol. 6:191–197.

Xavier KB, Bassler BL. 2005a. Interference with AI-2-mediated bacterial cell-cell communication. Nature 437:750–753.

Xavier KB, Bassler BL. 2005b. Regulation of uptake and processing of the quorum-sensing autoinducer AI-2 in *Escherichia coli*. J Bacteriol. 187: 238–248.

Zhu CC, et al. 2007. The possible influence of LuxS in the in vivo virulence of rabbit enteropathogenic *Escherichia coli*. Vet Microbiol. 125: 313–322.

**Associate editor:** Richard Cordaux